Decoherence of molecular vibrational wave packets: Observable manifestations and control criteria

C. Brif,[1,*] H. Rabitz,[1,†] S. Wallentowitz,[2,‡] and I. A. Walmsley[3,§]
[1]*Department of Chemistry, Princeton University, Princeton, New Jersey 08544*
[2]*Department of Physics and Astronomy and Rochester Theory Center for Optical Science and Engineering, University of Rochester, Rochester, New York 14627*
[3]*The Institute of Optics, University of Rochester, Rochester, New York 14627*
(Received 10 November 2000; published 7 May 2001)

Decoherence of molecular vibrational wave packets in hot alkaline dimers due to the vibration-rotation coupling is considered. The focus is on the study of observable manifestations of the decoherence process in molecular emission tomography. Criteria are presented for control over decoherence by means of driving molecular transitions with suitably shaped ultrafast laser pulses.

DOI: 10.1103/PhysRevA.63.063404 PACS number(s): 42.50.Hz, 32.80.Qk, 33.50.Dq, 07.05.Dz

I. INTRODUCTION

Any real system, no matter how well isolated, unavoidably interacts with the environment. This interaction makes evolution of a quantum system nonunitary and destroys coherence of quantum superpositions. This process, known as *decoherence* [1], is widely regarded as the most important and fundamental obstacle to the practical realization of quantum information processing [2–6].

A number of approaches have been proposed to overcome the decoherence problem. One principal approach employs quantum *error-correcting codes* [7–14] that include a variety of sophisticated schemes aimed to correct loss of information by monitoring the system and conditionally carrying on suitable feedback operations. Error-correcting codes allow fault-tolerant quantum computation provided that the error per operation is below a threshold value [6]. This threshold error rate should be quite low (it is estimated to be about 10^{-6} for quantum logic elements [6]). Therefore, a practical realization of quantum computation will likely require that fault-tolerant error-correcting codes be supplemented with a physical procedure able to significantly suppress the decoherence rate.

Another interesting approach [15–17] relies on the existence of decoherence-free subspaces of states that, due to special symmetry properties, are dynamically decoupled from the environment. Specifically, a decoherence-free subspace is the common eigenspace of an algebra of decoherence generators (operators by which the system is coupled to the environment). Quantum computation procedures that make use of the decoherence-free subspaces are called *error-avoiding codes* [18]. Unfortunately, error-avoiding codes have their own drawbacks. In practice, the complexity of multiparticle systems needed for scalable quantum computation may make the identification and use of decoherence-free subspaces extremely difficult, or such subspaces may not exist at all. Symmetry-based operations of error-avoiding codes may be impossible if the Hamiltonian of a complex quantum system is not completely known and/or if multiple decoherence mechanisms exist.

Along another line of research, a number of interesting works [19–23] analyzed schemes to counteract decoherence in quantum systems by applying sequences of frequent pulses. It was shown that a qubit (a two-level system) [20,21], a collection of qubits and a two-qubit quantum gate [21], and a quantum harmonic oscillator [22], coupled to a reservoir, may be made immune to decoherence if they are driven by a sequence of very fast pulses. In this approach, pulses of a suitable external field aim to reverse the sign of the interaction term in the Hamiltonian which describes the coupling to the reservoir. If the duration between successive pulses is much smaller than the typical reservoir time scale, than the effect of the interaction with the environment is effectively eliminated. An elegant group-theoretic generalization of this approach [23–25] shows that applied pulses are unitary transformations that form a finite-dimensional group, and the application of a series of pulses amounts to an average (symmetrization) over this group. This method (called *decoupling by symmetrization*) gives important physical insight into the issue of decoherence. However, a practical implementation of this approach to counteract decoherence in a realistic physical system may be problematic. An important technical problem is the need to use extremely short pulses at a very high rate. Another related problem is that the shorter the pulse duration, the more intense the field must be to perform the desired transformation. Apart from the technical issue of generating such intense fields, there exists a more fundamental problem: very strong driving fields will unavoidably induce undesirable nonlinear effects (e.g., multiphoton transitions, coupling to additional degrees of freedom, etc.), thereby affecting the most basic characteristics of the system.

The approaches mentioned above suffer from a problem that is generic to all *open-loop* control schemes: effective control requires complete *a priori* information about the sys-

*Electronic address: cbrif@princeton.edu
†Electronic address: hrabitz@chemvax.princeton.edu
‡Present address: Fachbereich Physik, Universität Rostock, Universitätsplatz 3, D-18051 Rostock, Germany. Electronic address: wal@physik5.uni-rostock.de
§Electronic address: walmsley@optics.rochester.edu

tem. For example, in order to identify the decoherence-free subspace or to design a cycle of pulses that will eliminate the coupling to the environment, it is necessary to know the decoherence generators. This issue is important because in practice, except for the simplest cases, detailed knowledge of the decoherence mechanisms is incomplete. Furthermore, the control field itself, if it is sufficiently intense, can modify the properties of the manipulated system in an uncontrolled way. Another serious difficulty is to find controls that are sufficiently robust to laboratory noise.

A natural and effective solution of all these problems is the use of *closed-loop* control methods [26,27], which iteratively adapt the form of the control field to manipulate the evolution of a complex quantum system in a desired way. In this approach, called *learning control*, results of measurements on the laser-driven quantum system are analyzed by an algorithm that evaluates the applied control field design and refines it, until the achieved result is as close as possible to the control objective. This approach takes advantage of a number of unique features: (a) the achieved control laser field is *optimal* for the *true* system Hamiltonian, complete knowledge of which is not required, (b) the design is robust to experimental disturbances and errors, and (c) the high-duty cycle of laser-pulse shaping is a rapidly evolving practical technology. Recent experiments [28–32] with atoms and molecules unequivocally demonstrated that closed-loop learning control is able to rapidly identify the ultrafast laser-pulses that are optimal for achieving a particular objective.

An interesting possibility is to use advanced methods of closed-loop quantum control with ultrafast laser pulses for optimally steering the dynamics of a quantum system towards the regions of low decoherence. In this paper, we lay the theoretical ground for future closed-loop control experiments by considering decoherence in a prototypical quantum system that is the vibrational degree of freedom of a diatomic molecule. An attractive feature of this system is the possibility to compare the theoretical analysis with closed-loop laboratory learning control experiments over the real molecule. Effective experimental tools have been developed for managing such systems [33]: there exists experimental capability to form various molecular wave packets and study their time evolution, including the complete characterization of the system density matrix.

Experiments performed with potassium and sodium dimers reveal that the main source of decoherence of the vibrational wave packets is the coupling between the vibrational mode and an effective thermal reservoir formed by the rotational levels of the molecule [33,34]. The theoretical analysis of this mechanism in the present paper is one of the basic steps towards the important goal of experimental realization of laboratory learning control over decoherence. As a forerunner to these developments, this paper mainly focuses on the study of observable effects of vibrational decoherence that are detectable by molecular emission tomography [33]. We consider manifestations of decoherence in the phase-space picture and in the time-resolved emission spectrum. The goal of this paper is to formulate control objectives and criteria to be used in closed-loop control over decoherence.

II. BASIC PROPERTIES OF THE SYSTEM

We consider the vibrational mode of an electronically excited potassium or sodium dimer and the vibration-rotation coupling that causes the decoherence of vibrational wave packets. In the Born-Oppenheimer approximation, the Hamiltonian describing the rovibrational nuclear motion for an electronic surface may be written as

$$\hat{H}=\left[\frac{\hat{p}^2}{2m}+V(\hat{q})\right]\otimes\hat{I}_r+\frac{\hbar^2}{2m}\hat{q}^{-2}\otimes\hat{\mathbf{J}}^2. \tag{1}$$

Here, $\hat{q}$ and $\hat{p}$ are the position and momentum operators for the internuclear separation, m is the reduced mass of the diatomic molecule ($m\simeq 19.48$ a.u. for the potassium dimer), $V(\hat{q})$ is the adiabatic potential surface for the given electronic state, $\hat{\mathbf{J}}$ is the (dimensionless) angular momentum operator, and $\hat{I}_r$ is the unit operator for the rotational degree of freedom. Expression (1) for the rovibrational Hamiltonian emphasizes that we consider the whole system as consisting of two coupled subsystems. The unitary evolution and quantum superpositions in the vibrational subsystem are disturbed due to the interaction with the rotational subsystem.

To capture the physical essence of the problem, we will consider only vibrational amplitudes that are sufficiently small, so that anharmonicities in the adiabatic potential may be neglected. Corrections to this approximation may be included in the theory and they will be naturally incorporated in the laboratory closed-loop decoherence control experiments. The harmonic potential is

$$V(\hat{q})=\epsilon_0-\tfrac{1}{2}\hbar\omega+\tfrac{1}{2}m\omega^2(\hat{q}-\overline{q})^2, \tag{2}$$

where ϵ_0 and ω are the vibrational ground-state energy and angular frequency, respectively, and $\overline{q}$ is the equilibrium internuclear separation (in the absence of rotations). It is useful to express the position and momentum in terms of bosonic annihilation and creation operators for the vibrational quanta, $\hat{q}=\overline{q}+q_0(\hat{a}+\hat{a}^\dagger)$, $\hat{p}=-ip_0(\hat{a}-\hat{a}^\dagger)$, where q_0 and p_0 are the position and momentum dispersions for the vibrational ground state. Then we obtain the usual harmonic expression for the vibrational part of the Hamiltonian,

$$\hat{H}_v=\frac{\hat{p}^2}{2m}+V(\hat{q})=\epsilon_0+\hbar\omega\hat{a}^\dagger\hat{a}. \tag{3}$$

Let us introduce a parameter, $\eta=q_0/\overline{q}$, which is a measure of the localization of the vibrations with respect to the equilibrium internuclear separation. For alkaline dimers, η is typically a small parameter, $\eta\ll 1$. Experimental values are $q_0\simeq 0.097$ Å, $\overline{q}\simeq 3.9$ Å, $\eta\simeq 0.025$, and $q_0\simeq 0.108$ Å, $\overline{q}\simeq 4.5$ Å, $\eta\simeq 0.024$ for the ground and first excited electronic states of the potassium dimer, respectively. Expanding $\hat{q}^{-2}$ around $\overline{q}$ to second order in η, we obtain

$$\hat{q}^{-2}\approx\overline{q}^{-2}[1-2\eta(\hat{a}+\hat{a}^\dagger)+3\eta^2(\hat{a}+\hat{a}^\dagger)^2]. \tag{4}$$

Substituting Eqs. (2) and (4) into the Hamiltonian (1), explicitly reveals the vibration-rotation coupling and identifies the decoherence generator for the vibrational mode. In the harmonic approximation, the rovibrational Hamiltonian (1) is given by

$$\hat{H}=\hat{H}_v\otimes\hat{I}_r+\hat{I}_v\otimes\hat{H}_r+\hat{H}_{\rm int}, \tag{5}$$

where $\hat{I}_v$ is the unit operator for the vibrational degree of freedom, $\hat{H}_v$ is the Hamiltonian for the vibrational subsystem [cf. Eq. (3)],

$$\hat{H}_r=\hbar B\hat{\mathbf{J}}^2 \tag{6}$$

is the Hamiltonian for the rotational subsystem, and

$$\hat{H}_{\rm int}=\hat{F}\otimes\hat{H}_r \tag{7}$$

is the interaction Hamiltonian. Here,

$$\hbar B=\hbar^2/(2m\overline{q^2}) \tag{8}$$

is the energy of the rotational quanta and

$$\hat{F}=6\eta^2\hat{a}^\dagger\hat{a}+3\eta^2(\hat{a}^2+\hat{a}^{\dagger 2})-2\eta(\hat{a}+\hat{a}^\dagger) \tag{9}$$

is the generator causing decoherence for the vibrational subsystem.

III. THE MECHANISM OF DECOHERENCE

In typical experiments, diatomic molecules of alkali metals are produced in a heat pipe. Therefore, the molecular ensemble is initially thermalized at a given temperature T (usually about 400 °C). Since the ratio of the vibrational to the rotational frequency ω/B is typically of the order of 10^3, the thermal energy is mainly contained in the rotational degree of freedom (experimental values are $\hbar\omega\simeq 1.2\times10^{-2}$ eV, $\hbar B\simeq 7.0\times10^{-6}$ eV, and $\hbar\omega\simeq 8.7\times10^{-3}$ eV, $\hbar B\simeq 5.2\times10^{-6}$ eV for the ground and first excited electronic states of the potassium dimer, respectively; the thermal energy is $k_BT\simeq 5.8\times10^{-2}$ eV). Consequently, we may assume that the initial uncorrelated state of the system is described by a density matrix of the form

$$\hat{\rho}(t_0)=\hat{\rho}_v(t_0)\otimes\hat{\rho}_r^{\rm th}, \tag{10}$$

where $\hat{\rho}_v(t_0)$ describes the initial state of the vibrational wave packet and

$$\hat{\rho}_r^{\rm th}=\sum_{j=0}^{\infty}p_j(T)\hat{\Pi}_j \tag{11}$$

is the thermal density matrix of the rotational subsystem. In Eq. (11), j is the quantum number of the angular momentum, with

$$\hat{\mathbf{J}}^2|j,m\rangle=j(j+1)|j,m\rangle,\quad \hat{J}_z|j,m\rangle=m|j,m\rangle, \tag{12}$$

$p_j(T)$ are the thermal-distribution probabilities,

$$p_j(T)=\mathcal{N}(2j+1)\exp\left[-\frac{\hbar Bj(j+1)}{k_BT}\right], \tag{13}$$

$\mathcal{N}$ is the normalization factor, and

$$\hat{\Pi}_j=\frac{1}{2j+1}\sum_{m=-j}^{j}|j,m\rangle\langle j,m| \tag{14}$$

are the projection operators on the invariant subspaces of given j.

Due to the interaction $\hat{H}_{\rm int}$ in Eq. (5), the vibrational and rotational subsystems become entangled and the phase information in the probability amplitudes of a vibrational quantum superposition decays. This rotational dephasing is the main source of decoherence found in the experiments with vibrational wave packets of sodium and potassium dimers [34]. It is convenient to study the effect of decoherence by considering the evolution of the vibrational subsystem in the Heisenberg picture. The expectation value of a time-dependent operator $\hat{A}(t)$ is given by

$$\langle\hat{A}(t)\rangle={\rm Tr}_v[\hat{\rho}_v(t_0)\langle\hat{A}(t)\rangle_{\rm rot}], \tag{15}$$

where ${\rm Tr}_v$ denotes the trace over the vibrational degree of freedom and $\langle\hat{A}(t)\rangle_{\rm rot}$ is the average over the thermal rotational distribution,

$$\langle\hat{A}(t)\rangle_{\rm rot}=\sum_{j=0}^{\infty}p_j(T)\hat{A}_j(t), \tag{16}$$

$$\hat{A}_j(t)={\rm Tr}[\hat{\Pi}_j\hat{A}(t)]. \tag{17}$$

Using the Hamiltonian (5), we obtain the Heisenberg equations of motion for the vibrational-mode operators $\hat{a}$ and $\hat{a}^\dagger$, which are combined to give

$$\left(\frac{d^2\hat{a}}{dt^2}+\omega^2\hat{a}\right)\otimes\hat{I}_r=\left(\frac{2\omega\eta}{\hbar}\hat{I}_v-\frac{12\omega\eta^2}{\hbar}\hat{a}\right)\otimes\hat{H}_r. \tag{18}$$

Projecting this equation on a subspace of given j, we find the equation of motion

$$\frac{d^2}{dt^2}\hat{a}_j+\Omega_j^2\hat{a}_j=h_j, \tag{19}$$

where $\Omega_j=\omega[1+2\lambda_j/\omega]^{1/2}$, $\lambda_j=6\eta^2Bj(j+1)$, and $h_j=2\eta\omega Bj(j+1)$. For temperatures about 400 °C, less than few hundred rotational levels are significantly excited. Therefore, $\lambda_j/\omega\ll 1$ for all the rotational levels of interest. Neglecting the terms of the order of $(\lambda_j/\omega)^2$ and smaller, as well as the displacement due to the free term h_j, we obtain the following approximate solution:

$$\hat{a}_j(t)=\hat{a}(0)e^{-i\omega t-i\lambda_j t}, \tag{20}$$

where we took for simplicity $t_0=0$. It is convenient to consider slowly varying bosonic operators in the frame that ro-

tates at the angular frequency ω (this is equivalent to working in the interaction picture with the free Hamiltonian $\hat{H}_0 = \hat{H}_v$). The solution in this rotating frame is simply $\hat{a}_j(t) = \hat{a}(0)\exp(-i\lambda_j t)$.

In order to average over the thermal rotational distribution, we need to evaluate the sum of Eq. (16). For sufficiently high temperatures ($\hbar B \ll k_B T$), it is a fair approximation to neglect the discreteness of the rotational spectrum and transform the sum over j into the integral over

$$x = \frac{\hbar B}{k_B T} j(j+1), \tag{21}$$

according to the formula

$$\sum_{j=0}^{\infty} p_j(T)\hat{A}_j(t) \rightarrow \int_0^{\infty} dx\, e^{-x}\hat{A}(x,t). \tag{22}$$

In the continuous limit, we have $\lambda_j \rightarrow \gamma x$, where

$$\gamma = 6\eta^2 k_B T/\hbar \tag{23}$$

is, as we will see shortly, the decoherence rate.

Using Eq. (20) and the continuous limit (22), it is easy to find the expression for the expectation value of a normally ordered product of the boson operators (in the rotating frame):

$$\langle \hat{a}^{\dagger m}(t)\hat{a}^n(t)\rangle = [1 + i(n-m)\gamma t]^{-1}\langle \hat{a}^{\dagger m}(0)\hat{a}^n(0)\rangle, \tag{24}$$

where m,n are non-negative integers. It is also interesting to consider the displacement operator,

$$\hat{D}(\xi,t) = \exp[\xi\hat{a}^{\dagger}(t) - \xi^*\hat{a}(t)] \tag{25}$$

(where $\xi \in \mathbb{C}$), and its expectation value,

$$\chi(\xi,t) = \mathrm{Tr}[\hat{\rho}_v \hat{D}(\xi,t)], \tag{26}$$

which is known as the characteristic function. Using the normal-ordering expansion of $\hat{D}(\xi,t)$, we find the time evolution of the characteristic function (in the rotating frame):

$$\chi(\xi,t) = e^{-|\xi|^2/2}\sum_{m=0}^{\infty}\sum_{n=0}^{\infty}\frac{\xi^m\xi^{*n}}{m!n!}\frac{\langle \hat{a}^{\dagger m}(0)\hat{a}^n(0)\rangle}{1 + i(n-m)\gamma t}. \tag{27}$$

This expression can be simplified, using the Fourier decomposition

$$\frac{1}{1 + i(n-m)\gamma t} = \int_0^{2\pi} d\phi P(\phi,t) e^{-i(n-m)\phi}, \tag{28}$$

where

$$P(\phi,t) = \frac{1}{2\pi}\sum_{k=-\infty}^{\infty}\frac{e^{ik\phi}}{1 + ik\gamma t} = \frac{\exp[-\phi/(\gamma t)]}{\gamma t[1 - e^{-2\pi/(\gamma t)}]}. \tag{29}$$

Then the time evolution of the characteristic function can be expressed in the following elegant form:

$$\chi(\xi,t) = \int_0^{2\pi} d\phi P(\phi,t)\chi(\xi e^{i\phi},0), \tag{30}$$

where $\chi(\xi,0)$ is the initial function and $P(\phi,t)$ acts as the decoherence kernel. Equation (30) implies that decoherence due to the vibration-rotation coupling appears as dephasing, i.e, the coupling smears the phase distribution of a vibrational wave packet. The characteristic time of this dephasing process is γ^{-1}. This should be compared to the vibrational period $T_0 = 2\pi/\omega$, which is typically 300–500 fs near the peak of the Franck-Condon transition (for the ground and first excited electronic states of the potassium dimer, T_0 is about 361 fs and 473 fs, respectively). At 400 °C, the decoherence rate γ is much smaller than the vibrational frequency (for the ground and first excited electronic states of the potassium dimer, $\gamma^{-1} \simeq 8.6T_0$ and $\gamma^{-1} \simeq 6.7T_0$, respectively).

Note that the above results for dephasing of vibrational states have been derived by neglecting the discrete nature of the rotational levels. If this discreteness is taken into account, the phase distribution of a vibrational wave packet, after being smeared to uniformity on the decoherence timescale γ^{-1}, will exhibit revivals on a much longer time scale. The time of the first revival is estimated as [34]

$$t_R = \frac{\pi}{\gamma}\sqrt{\frac{k_B T}{\hbar B}}. \tag{31}$$

For the potassium dimer at 400 °C, the ratio of the revival time t_R and the characteristic dephasing time γ^{-1} is of the order of 10^2. Consequently, the first revival would appear only after many hundreds of vibrational periods and is practically irrelevant in most experimental situations.

IV. TOWARDS CONTROL OF DECOHERENCE

Successful methods of control are determined by the physical properties of the system and, in the present case, by the properties of the decoherence generator $\hat{F}$ that couples the vibrational and rotational degrees of freedom. Inspecting the decoherence generator $\hat{F}$ of Eq. (9), reveals two important facts.

(i) $\hat{F}$ has no normalizable eigenstates. This is easy to see, because $\hat{F}$ is a function of the position operator $\hat{q} = \overline{q} + q_0(\hat{a} + \hat{a}^{\dagger})$ which has no normalizable eigenstates. Therefore, the decoherence-free subspace corresponding to $\hat{F}$ is null and the method of error-avoiding codes [15–18] is inapplicable.

(ii) $\hat{F}$ cannot be algebraically averaged out using the method of decoupling by symmetrization [23–25]. Roughly speaking, this happens because the part of $\hat{F}$ that is proportional to the number operator $\hat{a}^{\dagger}\hat{a}$ cannot be eliminated by the symmetrization procedure: the positiveness of the coefficient of $\hat{a}^{\dagger}\hat{a}$ is preserved under any closed group of transformations. A rigorous proof of this statement requires a de-

tailed account of the symmetrization procedure, which is beyond the scope of this paper, and will be presented elsewhere [35].

The above considerations indicate that neither of the open-loop schemes is applicable for control over vibrational decoherence in alkaline dimers. Therefore, an important avenue for the laboratory study will be to utilize modern control techniques to suppress decoherence, making use of ultrafast modulated laser pulses to drive transitions between the ground and excited electronic surfaces of the molecule. Although the molecular system under study does not support exact decoherence-free subspaces, closed-loop learning control should be able to identify the best possible low-decoherence evolution pathways. The present paper focuses on the study of observable manifestations of vibrational decoherence, in order to determine suitable control objectives to be used by the learning algorithm in the future experiments.

The laboratory study will be important to identify the principal physical mechanisms of decoherence control. A preliminary analysis shows that squeezing of a vibrational wave packet may be effective to decouple the vibrational mode from the rotational motion and thereby reduce decoherence. Physical intuition suggests that in order to implement the squeezing transformation, the control laser field should be adjusted to produce a parametric type of excitation, i.e., to drive transitions between vibrational levels that differ in energy by two vibrational quanta, $2\hbar\omega$. This excitation will guide the molecular evolution similarly to an effective squeezing-generating Hamiltonian quadratic in $\hat{a}$ and $\hat{a}^{\dagger}$. Also, the control field should be sufficiently fast to compensate for the free vibrational evolution $\hat{a}(t)=\hat{a}e^{-i\omega t}$. A detailed analysis of this mechanism of decoherence suppression will be presented elsewhere [35].

V. MANIFESTATIONS OF DECOHERENCE IN EMISSION TOMOGRAPHY

It should be emphasized that decisions made by the learning control algorithm are ultimately based on the chosen control objective. Moreover, a practical realization of closed-loop learning control in the laboratory requires an objective that can be easily deduced from the experimental data. An important experimental method that reveals the quantum dynamics of molecular vibrational wave packets is emission tomography [33]. Therefore, in this paper we focus on manifestations of decoherence in experimental data available via this measurement technique. The goal of this analysis is to determine a suitable control objective that may serve as a good measure of decoherence and is easily detected experimentally. This objective may then be used in the closed-loop laboratory experiments for exploring management of decoherence.

The standard detection technique employed in the method of emission tomography is time-resolved spectroscopy [33]. The time-dependent spontaneous emission spectrum from an excited diatomic molecule contains information about the vibrational wave packet on the excited electronic surface at a particular time. Specifically, the time-resolved spectroscopic data suffice to reconstruct the initial vibrational state of an ensemble of identically prepared molecules, provided that the potential energy surfaces for the ground and excited electronic states are known. The time gates used in the experiments have a duration of about 60 fs, which is much shorter than the vibrational period T_0 (typically 300–500 fs). Such a short time gate ensures that the vibrational wave packet does not move significantly during the time that the fluorescence is sampled. The spectrometer resolution is typically better than a few nanometers.

We consider two basic possibilities for tracking the effect of decoherence upon vibrational wave packets. One method makes use of phase-space distributions that may be reconstructed from the measured emission spectra. The phase-space picture of decoherence is very instructive and is widely used in theoretical and experimental studies. The other possibility is to monitor the effect of decoherence directly from the measured time-resolved spectrum. The former method is more intuitive, while the latter has a technical advantage since it does not require the reconstruction procedure.

A. Evidence of decoherence in the phase-space picture

Phase-space quasiprobability distributions for molecular vibrational states can be reconstructed from the time-resolved fluorescence spectrum via the inverse Radon transform [33]. These distributions contain all the information about the quantum state, and their form is sensitive to decoherence caused by the vibration-rotation coupling. The s-parametrized distributions are given by

$$W_s(\alpha,t)=\int_{\mathbb{C}}\frac{d^2\xi}{\pi}e^{s|\xi|^2/2}e^{\xi^*\alpha-\xi\alpha^*}\chi(\xi,t), \tag{32}$$

where $\chi(\xi,t)$ is the characteristic function of Eq. (26) and $\alpha\in\mathbb{C}$. The value of the parameter s of the phase-space distributions reconstructed in the emission tomography method depends on the experimental setup and the type of molecules used. The value of s indicates the degree to which the Wigner function (corresponding to $s=0$) is smoothed due to imperfections of the measurement procedure. Typical values of s are -0.7 and -0.3 for experiments with sodium and potassium dimers, respectively.

The effect of decoherence on the characteristic function is given by Eq. (30). Using this result and Eq. (32), it is easy to find how the phase-space distributions are affected by decoherence. The corresponding expression is similar to Eq. (30) and reads (in the rotating frame)

$$W_s(\alpha,t)=\int_0^{2\pi}d\phi P(\phi,t)W_s(\alpha e^{i\phi},0). \tag{33}$$

As we mentioned above, the decoherence rate γ is much smaller than the vibrational frequency in typical experiments with sodium and potassium dimers. Consequently, decoherence has little effect on the system during one vibrational period, which is the time interval needed to reconstruct the phase-space distribution of a quantum oscillator. This en-

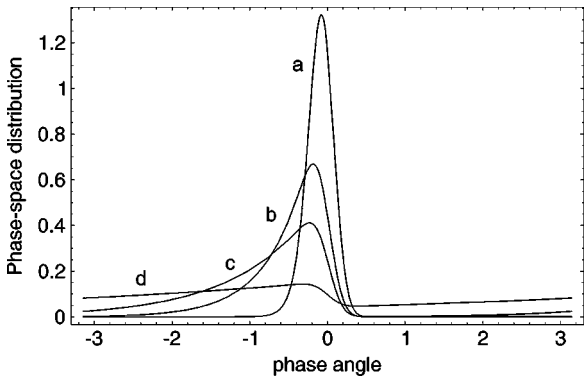

FIG. 1. The phase-space distribution $W_s(\alpha,t)$ for coherent state $|\beta\rangle$, with $|\alpha|=\beta=4.0$ and $s=-0.3$, versus arg α, at different times: (a) $\gamma t=0.1$, (b) $\gamma t=0.5$, (c) $\gamma t=1.0$, (d) $\gamma t=5.0$.

sures that phase-space distributions are correctly reconstructed by the emission tomography method. We will analyze the effect of decoherence by considering the time evolution of phase-space distributions for coherent states and coherent superpositions of the vibrational mode.

1. Dephasing of coherent states

Coherent states $|\beta\rangle$ are Gaussian wave packets with equal dispersion for position and momentum, which preserve their form during evolution in the harmonic potential. These states are produced by the action of the displacement operator on the ground state: $|\beta\rangle=\hat{D}(\beta)|0\rangle$, and an equivalent definition is $\hat{a}|\beta\rangle=\beta|\beta\rangle$. A simple calculation gives

$$\chi(\xi,0)=\langle\beta|\hat{D}(\xi,0)|\beta\rangle=e^{-|\xi|^2/2}e^{\beta^*\xi-\beta\xi^*}, \tag{34}$$

$$W_s(\alpha,0)=re^{-r|\alpha-\beta|^2}, \tag{35}$$

where $r=2/(1-s)$. The decoherence process of Eq. (33) smears the Gaussian distribution (35) along the ring of radius $|\beta|$ in the complex plane, thereby erasing the phase information. This process is illustrated in Fig. 1, where $W_s(\alpha,t)$ with $|\alpha|=\beta=4.0$ is plotted versus the phase angle argα at different times.

Dephasing of coherent states may be tracked by considering the decrease in the value of $W_s(\alpha,t)$ at the point $\alpha=\beta$ (which is initially the distribution maximum). The time dependence of this value is shown in Fig. 2 for different β. At very early times, for $\gamma t\ll 1$ and $\gamma t|\beta|\ll 1$, we find that $W_s(\beta,t)$ decreases as

$$W_s(\beta,t)\approx r[1-2r|\beta|^2(\gamma t)^2], \tag{36}$$

and at very long times, for $\gamma t\gg 1$, it reaches a constant value,

$$W_s(\beta,t)\approx re^{-2r|\beta|^2}I_0(2r|\beta|^2)\approx\sqrt{r/(4\pi)}|\beta|^{-1}. \tag{37}$$

Here, $I_0(z)$ is the modified Bessel function of the first kind, and the last approximation is valid for $|\beta|^2\gg 1$. This saturation at long times corresponds to the complete randomization of the phase distribution.

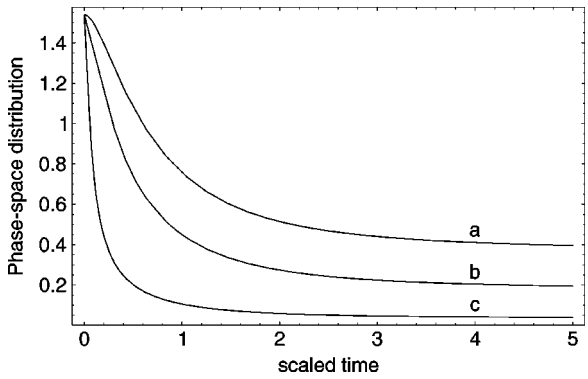

FIG. 2. The phase-space distribution $W_s(\alpha,t)$ for coherent state $|\beta\rangle$, with $\alpha=\beta$ and $s=-0.3$, versus γt, for (a) $\beta=1.0$, (b) $\beta=2.0$, (c) $\beta=10.0$.

2. Dephasing of coherent superpositions

We consider the superposition of coherent states (also known as Schrödinger's cat) of the form

$$|\beta,v\rangle=\mathcal{N}(|\beta\rangle+e^{iv}|-\beta\rangle), \tag{38}$$

$$\mathcal{N}=[2(1+e^{-2|\beta|^2}\cos v)]^{-1/2}. \tag{39}$$

The characteristic function and the phase-space distribution are

$$\chi(\xi,0)=\mathcal{N}^2[e^{-|\xi|^2/2}(e^{\beta^*\xi-\beta\xi^*}+e^{\beta\xi^*-\beta^*\xi})+e^{iv}e^{-|\xi-2\beta|^2/2}+e^{-iv}e^{-|\xi+2\beta|^2/2}], \tag{40}$$

$$W_s(\alpha,0)=r\mathcal{N}^2[e^{-r|\alpha-\beta|^2}+e^{-r|\alpha+\beta|^2}+e^{-2|\beta|^2}(e^{iv}e^{-r(\alpha-\beta)^*(\alpha+\beta)}+\text{c.c.})]. \tag{41}$$

For the coherent superpositions $|\beta,v\rangle$, the process of dephasing occurs in a manner very similar to what was seen for the coherent states. The loss of the phase information for the even superposition $|\beta,0\rangle$ is illustrated in Fig. 3, where $W_s(\alpha,t)$ with $|\alpha|=\beta=4.0$ is plotted versus arg α at different times.

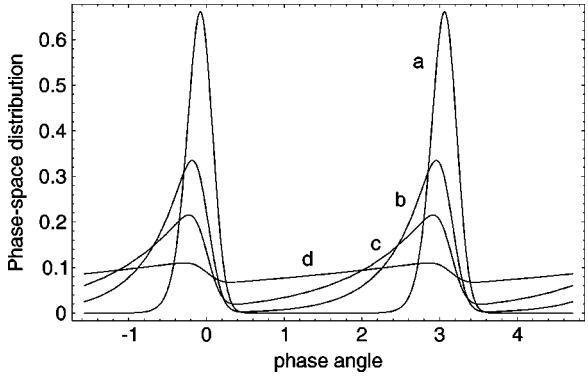

FIG. 3. The phase-space distribution $W_s(\alpha,t)$ for even coherent superposition $|\beta,0\rangle$, with $|\alpha|=\beta=4.0$ and $s=-0.3$, versus arg α, at different times: (a) $\gamma t=0.1$, (b) $\gamma t=0.5$, (c) $\gamma t=1.0$, (d) $\gamma t=5.0$.

Dephasing of coherent superpositions may be tracked by considering the decrease in the value of $W_s(\alpha,t)$ at the point $\alpha=\beta$ (at one of the two maxima of the initial distribution). The time dependence of this value is very similar to what was found for the coherent states (see Fig. 2). At very early times, for $\gamma t \ll 1$ and $\gamma t|\beta| \ll 1$, and for large amplitudes, $|\beta|^2 \gg 1$, we find that $W_s(\beta,t)$ decreases as

$$W_s(\beta,t) \approx (r/2)[1-2r|\beta|^2(\gamma t)^2], \tag{42}$$

and at very long times, for $\gamma t \gg 1$, it reaches a constant value,

$$\begin{aligned} W_s(\beta,t) &\approx 2r\mathcal{N}^2[e^{-2r|\beta|^2} I_0(2r|\beta|^2) \\ &\quad + e^{-2|\beta|^2} J_0(2r|\beta|^2)\cos v] \\ &\approx \sqrt{r/(4\pi)}\,|\beta|^{-1}. \end{aligned} \tag{43}$$

Here, $J_0(z)$ is the Bessel function of the first kind, and the last approximation in Eq. (43) is valid for $|\beta|^2 \gg 1$.

In theoretical studies, decoherence of coherent superpositions is often estimated from the value of the characteristic function $\chi(\xi,t)$ at the point $\xi=2\beta$ (or $\xi=-2\beta$). As is seen from Eq. (40), one of the interference terms in $\chi(\pm 2\beta,0)$ is of the order of unity, while the other terms are exponentially small for $|\beta|^2 \gg 1$. As the interferences are destroyed in the decoherence process, $\chi(\pm 2\beta,t)$ rapidly decays. The time dependence of $\chi(2\beta,t)$ for the even superposition $|\beta,0\rangle$ is very similar to that of the initial distribution maximum $W_s(\beta,t)$. At very early times, for $\gamma t \ll 1$ and $\gamma t|\beta| \ll 1$, and for large amplitudes, $|\beta|^2 \gg 1$, the characteristic function of the even superposition $|\beta,0\rangle$ decreases as

$$\chi(2\beta,t) \approx (1/2)[1-4|\beta|^2(\gamma t)^2], \tag{44}$$

and at very long times, for $\gamma t \gg 1$, it reaches a constant value,

$$\begin{aligned} \chi(2\beta,t) &\approx 2\mathcal{N}^2[e^{-4|\beta|^2} I_0(4|\beta|^2) + e^{-2|\beta|^2} J_0(4|\beta|^2)] \\ &\approx \sqrt{1/(8\pi)}\,|\beta|^{-1}, \end{aligned} \tag{45}$$

where the last approximation is valid for $|\beta|^2 \gg 1$.

3. Phase-space overlap as a control criterion

The value $W_s(\beta,t)$ of the initial distribution maximum may be a good measure of decoherence for coherent states or coherent superpositions. However, the tracking of this value may be insufficient if our aim is not just to suppress dephasing, but to control the quantum state of the vibrational mode in a more detailed manner. Let the target state at time t be $\tilde{\rho}(t)$, with the phase-space distribution $\tilde{W}_s(\alpha,t)$, and the actual state at time t be $\hat{\rho}(t)$, with the phase-space distribution $W_s(\alpha,t)$. Then we may control the state using the phase-space overlap of the target distribution $\tilde{W}_s(\alpha,t)$ and the measured distribution $W_s(\alpha,t)$. We consider the overlap functional of the form

$$\mathcal{J}_s[\tilde{\rho}(t),\hat{\rho}(t)] = \int_{\mathrm{C}} \frac{d^2\alpha}{\pi} [\tilde{W}_s(\alpha,t) W_s(\alpha,t)]^{1/2}, \tag{46}$$

which satisfies $\mathcal{J}_s=1$ for $\hat{\rho}(t)=\tilde{\rho}(t)$.

As an example, we consider the time dependence of $\mathcal{J}_s$ when the target is the coherent state $|\beta\rangle$, which is also the initial state thermally dephased according to the model (33). Then we obtain (we continue to use the rotating frame):

$$\begin{aligned} \mathcal{J}_s(t) &= \int_0^{2\pi} d\phi P(\phi,t) \int_{\mathrm{C}} \frac{d^2\alpha}{\pi} r e^{-r|\alpha-\beta|^2/2 - r|\alpha e^{i\phi}-\beta|^2/2} \\ &= \int_0^{2\pi} d\phi P(\phi,t) \exp[-r|\beta|^2 \sin^2(\phi/2)]. \end{aligned} \tag{47}$$

The behavior of the overlap $\mathcal{J}_s(t)$ in this case is very similar to what we found for the initial distribution maximum $W_s(\beta,t)$ (see Fig. 2). At very early times, for $\gamma t \ll 1$ and $\gamma t|\beta| \ll 1$, the overlap decreases as

$$\mathcal{J}_s(t) \approx 1-(r/2)|\beta|^2(\gamma t)^2, \tag{48}$$

and at very long times, for $\gamma t \gg 1$, it reaches a constant value,

$$\mathcal{J}_s(t) \approx e^{-r|\beta|^2/2} I_0(r|\beta|^2/2) \approx \sqrt{1/(r\pi)}\,|\beta|^{-1}, \tag{49}$$

where the last approximation is valid for $|\beta|^2 \gg 1$.

The above results indicate that the phase-space picture is suitable for tracking the effect of decoherence on vibrational wave packets. Dephasing of phase-space distributions, as well as related changes in density-matrix elements and phase-space overlaps, will be especially useful as control criteria for the theoretical analysis of optimal control over decoherence.

B. Evidence of decoherence in the emission spectrum

Although the phase-space picture of decoherence is very instructive, relying on phase-space distributions (or on density-matrix elements) requires a computationally complicated reconstruction procedure (based on the inverse Radon transform). This issue is especially relevant when considering closed-loop laboratory control experiments in which it is desirable to keep off-line computation to a minimum. An alternative way to track the influence of decoherence is to directly monitor the measured spectrum. The spontaneous radiation from an ensemble of molecules may be sampled using a time gate that allows all of the radiation through in a short time window (of duration Γ^{-1}) near a time t, and the spectrum of this temporal slice of fluorescence is then measured by a spectrometer with bandpass centered at frequency Ω. The measured spectrum $S(\Omega,t)$ may be written in terms of the normally ordered two-time correlation function of the electric-field operator. Using the Schrödinger picture, one can express $S(\Omega,t)$ as the time-dependent expectation value of an operator $\hat{O}(\Omega)$, and the phase-space representation of this expectation value is

$$S(\Omega,t) = \int_{\mathrm{C}} \frac{d^2\alpha}{\pi} O_{-s}(\alpha;\Omega) W_s(\alpha,t). \tag{50}$$

Within the harmonic approximation, the phase-space function $O_{-s}(\alpha;\Omega)$ can be calculated analytically [33]:

$$O_{-s}(\alpha;\Omega)=\frac{1}{\sqrt{\pi(s-s_m)}}\exp\left\{-\frac{[q-Q(\Omega)]^2}{s-s_m}\right\}. \quad (51)$$

Here, $q=\sqrt{2}\,\mathrm{Re}\,\alpha$, $Q(\Omega)=(\Omega-\kappa^2\omega)/(\sqrt{2}\kappa\omega)$ is the mapping of position to emitted frequency, $\kappa=(\bar{q}_e-\bar{q}_g)/q_0$ is the ratio of the displacement of the potential minima (for the excited and ground electronic surfaces) to the vibrational ground-state width, and $s_m=-(\Gamma/\kappa\omega)^2$. The above result is valid under the assumption $\omega/\Gamma\ll 1$ (i.e., the time gate must be short compared to the vibrational period), but on the other hand, one needs to keep the time window sufficiently wide to allow for accurate spectroscopy (in the phase-space picture this is equivalent to the requirement $|s_m|<1$, so the reconstructed phase-space distribution will not be too smoothed). The function $O_{-s}(\alpha;\Omega)$ is a Gaussian distribution of Q and converges to the Dirac delta distribution for $s\to s_m$. The prefactor in Eq. (51) is chosen to keep $O_{-s}(\alpha;\Omega)$ and $S(\Omega,t)$ normalized to unit distributions of Q.

If the vibrational wave packet evolves freely without decoherence, then the spectrum is

$$S_0(\Omega,t)=\int_{\mathbb{C}}\frac{d^2\alpha}{\pi}O_{-s}(\alpha;\Omega)W_s(\alpha e^{i\omega t}). \quad (52)$$

Taking into account the decoherence process of the form (33), we obtain the following expression for the time-dependent spectrum:

$$S(\Omega,t)=\int_0^{2\pi}d\phi P(\phi,t)S_0(\Omega,t+\phi/\omega). \quad (53)$$

The above result may be used to study how decoherence affects the spectrum. As an illustrative example, we consider dephasing of a coherent state $|\beta\rangle$. The decoherence-free spectrum for the coherent state $|\beta\rangle$ is obtained by substituting the Wigner function (35) and expression (51) into Eq. (52). Carrying out the integration, we find

$$S_0(\Omega,t)=\frac{1}{\sqrt{\pi(1-s_m)}}\exp\left\{-\frac{[q_\beta(t)-Q(\Omega)]^2}{1-s_m}\right\}, \quad (54)$$

where $q_\beta(t)=\sqrt{2}\,\mathrm{Re}(\beta e^{-i\omega t})$. The spectrum in Eq. (54) is a Gaussian distribution in Q, whose standard deviation is $\sigma=\sqrt{(1-s_m)/2}$, and the center $q_\beta(t)$ oscillates periodically with t. Using Eq. (53), we explore numerically the effect of rotational dephasing on this spectrum (for illustration here we take $\gamma^{-1}=8T_0$ and $s_m=-0.3$ which are typical values for experiments with the potassium dimer). Figure 4 shows $S(\Omega,t)$ for $\beta=4.0$ versus Q at different times. At very long times, for $\gamma t\gg 1$, dephasing produces a distribution symmetric about $Q=0$, with two equal maxima at $Q=\pm\sqrt{2}|\beta|$. This long-time asymptotic spectrum, $S(\Omega,t)$ for $\gamma t=50$, is plotted in Fig. 5 versus Q for different β. The above results indicate that the time-dependent emission spectrum $S(\Omega,t)$ is quite sensitive to decoherence induced by the vibration-rotation coupling. Consequently, the directly observable change in the measured spectrum is a suitable control criterion for laboratory learning control over vibrational decoherence.

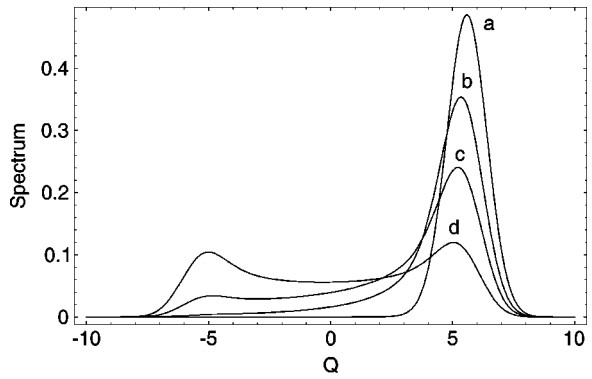

FIG. 4. The spectrum $S(\Omega,t)$ for dephasing of coherent state $|\beta\rangle$, with $\beta=4.0$, $s_m=-0.3$, and $\gamma^{-1}=8T_0$, versus the scaled frequency Q, at different times: (a) $t=T_0$, (b) $t=4T_0$, (c) $t=8T_0$, (d) $t=40T_0$.

VI. CONCLUSIONS

In this paper we studied decoherence of molecular vibrational wave packets in hot alkaline dimers. Decoherence caused by the vibration-rotation coupling appears as dephasing, i.e., the interaction erases the phase information of a vibrational quantum state. For hot molecules ($k_BT\gg\hbar B$), the decoherence rate is proportional to the temperature. However, for temperatures about 400 °C (which is typical for experiments with sodium and potassium dimers), the decoherence rate is much smaller than the vibrational frequency, which ensures that the vibrational state can be correctly reconstructed via the emission tomography method.

We presented the concepts of closed-loop learning control over decoherence. In this control method, decoherence of vibrational wave packets may be suppressed by driving the transitions between the ground and excited electronic surfaces of the molecule with suitably shaped ultrafast laser pulses. Theoretically, the optimal shape of the laser pulse can be obtained by minimizing a cost functional that includes the control objective and physically significant restrictions on

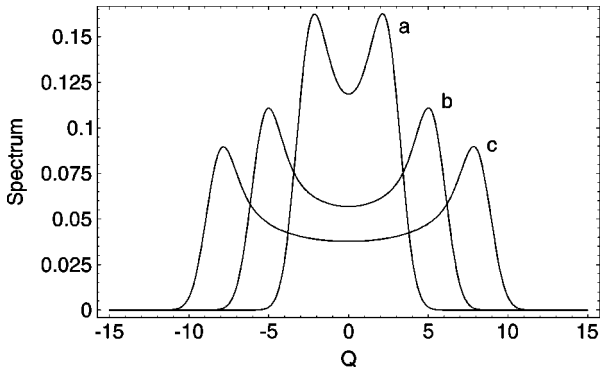

FIG. 5. The long-time spectrum $S(\Omega,t)$ for dephasing of coherent state $|\beta\rangle$, with $s_m=-0.3$, $\gamma^{-1}=8T_0$, and $\gamma t=50$, versus the scaled frequency Q, for (a) $\beta=2.0$, (b) $\beta=4.0$, (c) $\beta=6.0$.

the laser field and/or the molecular dynamics. Experimentally, it is preferable to use closed-loop laboratory control with a learning algorithm that singles out the pulse shape that is most suitable for decoherence suppression. The vibrational mode of an electronically excited alkaline dimer is ideal for application of the learning control method, since it is a system where a very precise comparison of theoretical predictions and experimental results can be made. The basic open question concerns the degree to which decoherence may be suppressed by control.

Laboratory learning control aims to optimize an objective that is a sensitive measure of decoherence and is easily measured in a realistic experiment. In our analysis we assumed that the information about the vibrational wave packet is obtained by the emission tomography method that employs time-resolved spectroscopy data. These data can be inverted to obtain phase-space quasiprobability distributions that contain all the information about the vibrational state. We studied the manifestations of decoherence in the phase-space picture. This study shows that the change induced by decoherence in the phase-space distributions is a very suitable control criterion for theoretical optimal control analysis. However, the use of this decoherence measure requires the time-consuming inversion procedure that may slow down the work of the learning algorithm in closed-loop laboratory control. Therefore, we studied the effect of decoherence on the time-resolved emission spectrum that is directly measured in the experiment. Our analysis shows that the form of the spectrum is a sensitive measure of decoherence that is suitable for use in laboratory learning control. In fact, tracking of decoherence by its directly observable effect on the spectrum may be accompanied by the reconstruction of the phase-space distribution representing the vibrational state. This will provide a very detailed comparison of the theoretically derived and experimentally achieved target states, and so help us to understand whether the employed theoretical model of the vibration-rotation coupling is adequate.

ACKNOWLEDGMENTS

This work was supported by the NSF and DOD. S.W. acknowledges support by the Studienstiftung des Deutschen Volkes.

[1] W. H. Zurek, Phys. Rev. D **24**, 1516 (1981); **26**, 1862 (1982); Phys. Today **44**(10), 36 (1991).
[2] I. L. Chuang, R. Laflamme, P. W. Shor, and W. H. Zurek, Science **270**, 1633 (1995).
[3] W. G. Unruh, Phys. Rev. A **51**, 992 (1995).
[4] G. M. Palma, K.-A. Suominen, and A. K. Ekert, Proc. R. Soc. London, Ser. A **452**, 567 (1996).
[5] C. H. Bennett and P. W. Shor, IEEE Trans. Inf. Theory **44**, 2724 (1998).
[6] E. Knill, R. Laflamme, and W. H. Zurek, Science **279**, 342 (1998).
[7] P. W. Shor, Phys. Rev. A **52**, R2493 (1995).
[8] A. Ekert and C. Macchiavello, Phys. Rev. Lett. **77**, 2585 (1996).
[9] D. P. DiVincenzo and P. W. Shor, Phys. Rev. Lett. **77**, 3260 (1996).
[10] A. R. Calderbank and P. W. Shor, Phys. Rev. A **54**, 1098 (1996).
[11] A. R. Calderbank, E. M. Rains, P. W. Shor, and N. J. A. Sloane, Phys. Rev. Lett. **78**, 405 (1997).
[12] A. M. Steane, Philos. Trans. R. Soc. London, Ser. A **356**, 1739 (1998).
[13] A. M. Steane, Nature (London) **399**, 124 (1999).
[14] D. G. Cory, M. D. Price, W. Maas, E. Knill, R. Laflamme, W. H. Zurek, T. F. Havel, and S. S. Somaroo, Phys. Rev. Lett. **81**, 2152 (1998).
[15] P. Zanardi and M. Rasetti, Phys. Rev. Lett. **79**, 3306 (1997); P. Zanardi, Phys. Rev. A **56**, 4445 (1997); **57**, 3276 (1998); **60**, R729 (1999).
[16] D. A. Lidar, I. L. Chuang, and K. B. Whaley, Phys. Rev. Lett. **81**, 2594 (1998); D. A. Lidar, D. Bacon, and K. B. Whaley, *ibid.* **82**, 4556 (1999); D. Bacon, J. Kempe, D. A. Lidar, and K. B. Whaley, *ibid.* **85**, 1758 (2000); D. Bacon, D. A. Lidar, and K. B. Whaley, Phys. Rev. A **60**, 1944 (1999): D. A. Lidar, D. Bacon, J. Kempe, and K. B. Whaley, *ibid.* **61**, 052307 (2000); D. A. Lidar, D. Bacon, J. Kempe, and K. B. Whaley, *ibid.* **63**, 022306 (2001); **63**, 022307 (2001).
[17] L.-M. Duan and G.-C. Guo, Phys. Rev. Lett. **79**, 1953 (1997); Phys. Rev. A **57**, 737 (1998); Phys. Lett. A **243**, 265 (1998).
[18] L.-M. Duan and G.-C. Guo, Phys. Lett. A **255**, 209 (1999).
[19] N. Imoto, Prog. Cryst. Growth Charact. Mater. **33**, 295 (1996).
[20] L. Viola and S. Lloyd, Phys. Rev. A **58**, 2733 (1998).
[21] L.-M. Duan and G.-C. Guo, Phys. Lett. A **261**, 139 (1999).
[22] D. Vitali and P. Tombesi, Phys. Rev. A **59**, 4178 (1999).
[23] L. Viola, E. Knill, and S. Lloyd, Phys. Rev. Lett. **82**, 2417 (1999).
[24] L. Viola, S. Lloyd, and E. Knill, Phys. Rev. Lett. **83**, 4888 (1999); L. Viola, E. Knill, and S. Lloyd, *ibid.* **85**, 3520 (2000).
[25] P. Zanardi, Phys. Lett. A **258**, 77 (1999); Phys. Rev. A **63**, 012301 (2001).
[26] R. S. Judson and H. Rabitz, Phys. Rev. Lett. **68**, 1500 (1992).
[27] H. Rabitz, R. de Vivie-Riedle, M. Motzkus, and K. Kompa, Science **288**, 824 (2000).
[28] C. J. Bardeen, V. V. Yakovlev, K. R. Wilson, S. D. Carpenter, P. M. Weber, and W. S. Warren, Chem. Phys. Lett. **280**, 151 (1997).
[29] A. Assion, T. Baumert, M. Bergt, T. Brixner, B. Kiefer, V. Seyfried, M. Strehle, and G. Gerber, Science **282**, 919 (1998).
[30] T. C. Weinacht, J. Ahn, and P. H. Bucksbaum, Nature (London) **397**, 233 (1999).
[31] R. Bartels, S. Backus, E. Zeek, L. Misoguti, G. Vdovin, I. P. Christov, M. M. Murnane, and H. C. Kapteyn, Nature (London) **406**, 164 (2000).
[32] B. J. Pearson, J. L. White, T. C. Weinacht, and P. H. Bucksbaum, Phys. Rev. A (to be published).
[33] I. A. Walmsley and L. Waxer, J. Phys. B **31**, 1825 (1998).
[34] S. Wallentowitz, I. A. Walmsley, and L. Waxer (unpublished).
[35] C. Brif, H. Rabitz, S. Wallentowitz, and I. A. Walmsley (unpublished).